Biochemical Pharmacology 78 (2009) 390–395

Contents lists available at ScienceDirect

Biochemical Pharmacology

journal homepage: www.elsevier.com/locate/biochempharm

Reduced skin inflammatory response in mice lacking inducible nitric oxide synthase

Rodrigo Medeiros, Cláudia P. Figueiredo, Giselle F. Passos, João B. Calixto *

Departamento de Farmacologia, Centro de Ciências Biológicas, Universidade Federal de Santa Catarina, Santa Catarina, Brazil

ARTICLE INFO

Article history:
Received 6 March 2009
Accepted 14 April 2009

Keywords:
Skin
Inflammation
Inducible nitric oxide synthase
Cyclooxygenase-2
12-O-tetradecanoylphorbol-13-acetate

ABSTRACT

The skin is the largest organ in the body and one of its main functions is to protect the body from environmental and endogenous noxious conditions, such as injury, infection and inflammation. The inducible nitric oxide synthase (iNOS) has been implicated as a key component in the inflammatory response. In the present study, we assessed the role of iNOS in the skin inflammation induced by 12-O-tetradecanoylphorbol-13-acetate (TPA). Mice deficient in iNOS had reduced edema and cellular infiltration in the skin following topical TPA application. Moreover, the genetic blockage of iNOS signaling inhibited the TPA-induced ERK and p38 activation resulting in reduced COX-2 upregulation. Finally, immunohistochemical studies revealed that iNOS knockout mice exhibited marked inhibition of AP-1, CREB and NF-κB transcriptional factors activation. Together, these results indicate that TPA induces the activation of several iNOS-dependent intracellular signaling pathways that have a key role in the control of inflammatory response in the skin. Therefore, selective iNOS inhibitors may be potentially relevant tools for cutaneous skin disease drug development.

1. Introduction

The nitric oxide synthase (NOS) catalyses the oxidation of the amino acid L-arginine to produces nitric oxide (NO). Molecular cloning and sequence analysis have revealed the existence of three distinct NOS isotypes [1]. The neuronal NOS (nNOS, NOS1) and endothelial NOS (eNOS, NOS3), are normally constitutively expressed. They generate only small amounts of NO that are sufficient for cellular signaling under most circumstances [2]. Conversely, the third type of NOS (iNOS, NOS2) is inducible by noxious conditions, such as injury, infection and inflammation, and is able to generate large amounts of NO [3]. While moderate levels of iNOS-derived NO are beneficial in principal, in contrast, overexpression of iNOS has been associated with most acute and chronic disorders, e.g., septic and hemorrhagic shock, liver injury, Alzheimer's disease, and tumors [4–7].

Inflammation is a complex biological response of the host immune system to injurious stimuli. There are amount of experimental evidence indicating that exposure of skin to 12-O-tetradecanoylphorbol-13-acetate (TPA) promotes intense local inflammation that activates multiple immunostimulatory pathways similar to that found in typical skin diseases including psoriasis, skin tumors and atopic dermatitis [8–10]. Furthermore, the skin inflammatory response elicited by TPA is now known to be associated with an activation of several intracellular pathways, e.g. mitogen-activated protein kinases (MAPKs), nuclear factor-κB (NF-κB) and, activator protein-1 (AP-1), as well as an increase in the content chemical mediators, such as cytokines, chemokines, vasoactive peptides, prostaglandins, leukotrienes and, NO, among others [11–14].

In the present study, we analyzed the role of iNOS in the skin inflammatory response induced by TPA in mice. Data presented indicate that mice lacking the iNOS exhibit consistent reduction of TPA-induced skin inflammation as assessed by reduction in skin edema and granulocyte infiltration. Likewise, we have demonstrated the involvement of iNOS in the activation of downstream signaling proteins, mainly MAPKs, c-Jun, NF-κB and cyclic AMP (cAMP)-response element-binding (CREB), as well as on the upregulation of cyclooxygenase-2 (COX-2) expression following topical application of TPA.

2. Materials and methods

2.1. Animals

Experiments were conducted using 3-month-old male C57Bl/6 (WT) and iNOS knockout ($iNOS^{-/-}$) mice kept in a controlled room temperature (22 ± 2 °C) and humidity (60–80%) under a 12 h light/

* Corresponding author at: Departamento de Farmacologia, Universidade Federal de Santa Catarina, Campus Universitário, Trindade, Bloco D, CCB, Caixa Postal 476, CEP 88049-900, Florianópolis, SC, Brazil. Tel.: +55 48 3721 9491/55 48 3721 9764; fax: +55 48 3337 5479.
E-mail addresses: calixto@farmaco.ufsc.br, calixto3@terra.com.br (J.B. Calixto).

0006-2952/$ – see front matter © 2009 Elsevier Inc. All rights reserved.
doi:10.1016/j.bcp.2009.04.021

dark cycle (lights on 6:00 A.M.). The iNOS$^{-/-}$ mice are on the C57Bl/6 background, constructed as described previously [15]. All procedures used in the present study followed the "Principles of Laboratory Animal Care" from National Institutes of Health (NIH) publication number 85–23 and were approved by the Animal Ethics Committee of the Universidade Federal de Santa Catarina.

2.2. TPA induced skin inflammation and ear edema measurement

The skin inflammation was induced in the right ear by the topical application of 2.5 μg/ear of TPA dissolved in 20 μl of acetone. Control animals received the same volume of acetone (vehicle) in the right ear. The ear edema was assessed at 2, 4 and 6 h after TPA application and was expressed as the increase in ear thickness due to the inflammatory challenge. Ear thickness was measured before and after induction of the inflammatory response by using a micrometer (Mitutoyo, Suzano, SP, Brazil) that was applied near the tip of the ear just distal to the cartilaginous ridges and the thickness was recorded in μm. To minimize variation due to technique, a single investigator performed the measurements throughout any one experiment.

2.3. Western blot

The western blot analyses were carried out in 6 mm punch-biopsies obtained from the mice ear. Tissues were homogenized in ice-cold 10 mM HEPES (pH 7.4), containing 1.5 mM $MgCl_2$, 10 mM KCl, 1 mM phenylmethylsulphonyl fluoride, 5 μg/ml leupeptin, 5 μg/ml pepstatin A, 10 μg/ml aprotinin, 1 mM sodium orthovanadate, 10 mM β-glycerophosphate, 50 mM sodium fluoride, 0.5 mM dithiothreitol and 1% Triton X-100. The homogenates were chilled on ice under vigorous shaking for 15 min and then centrifuged at 14,000 × *g* for 60 min at 4 °C. The supernatant was aliquoted and stored at −70 °C. The protein concentration was determined using the protein assay kit according to the manufacturer's instructions (Bio-Rad, São Paulo, SP, Brazil).

Equal protein amounts were separated on a SDS-PAGE, and then transferred to a polyvynilidene fluoride membrane (Immobilon P; Millipore, Bedford, MA, USA). The membranes were saturated by incubation with 10% non-fat dry milk solution and then incubated overnight with p38 (1:1000), ERK (1:2000), β-actin (1:1000), iNOS (1:5000), COX-2 (1:10 000), phosphorylated (p)-p38(Thr^{180} and Tyr^{182}) (1:2000), or p-ERK(Thr^{183} and Tyr^{185}) (1:5000) antibody. Following washing, the membranes were incubated with adjusted secondary antibodies coupled to horseradish peroxidase or alkaline phosphatase. The immunocomplexes were visualized using the ECL chemiluminescence detection system or 5-bromo-4-chloro-3-indolyl phosphate/nitroblue tetrazolium color development substrate (BCIP/NBT). Band density measurements were made using NIH ImageJ 1.36b imaging software (NIH, Bethesda, MD, USA).

2.4. Histopathological and immunohistochemical studies

Ear samples were collected and fixed in a phosphate buffered saline (PBS) solution containing 4% paraformaldehyde for 24 h at room temperature, dehydrated by graded ethanol, and embedded in paraffin. For histological evaluation, tissue sections (5 μm) were deparaffinized with xylene and stained using hematoxylin and eosin.

Immunohistochemistry was carried out on paraffin tissue sections using the p-CREB(Ser^{133}) (1:100), p-c-Jun(Ser^{73}) (1:50), p-p65 NF-κB(Ser^{276}) (1:100), iNOS (1:100) or COX-2 (1:200) antibody. Following quenching of endogenous peroxidase with 1.5% hydrogen peroxide in methanol (v/v) for 20 min, high temperature antigen retrieval was performed by immersion of the slides in a water bath at 95–98 °C in 10 mM trisodium citrate buffer pH 6.0, for 45 min. The slides were then processed using the Vectastain Elite ABC reagent according to the manufacturer's instructions. Following the appropriate biotinylated secondary antibody, sections were developed with DAB (3,3′-diaminobenzidine) in chromogen solution for the exact amount of time and counterstained with Harris's hematoxylin. Control and experimental tissues were placed on the same slide and processed under the same conditions.

Images of skin sections stained with hematoxylin and eosin, or antibodies to p-CREB, p-c-Jun, p-p65 NF-κB, or COX-2 were acquired using a Sight DS-5M-L1 digital camera connected to an Eclipse 50i light microscope (both from Nikon, Melville, NY, USA). Infiltrating inflammatory cells and p-CREB, p-c-Jun, or p-p65 NF-κB immunostaining were determined upon visual inspection in a masked fashion by counting the labeled cells in four non-coincident fields using a counting grid at 400× magnification. The numbers of infiltrating inflammatory cells obtained per field were averaged. The p-CREB, p-c-Jun and p-p65 NF-κB immunostaining were expressed as the percentage of positive cells.

2.5. Reagents

The following substances were used: 12-O-tetradecanoylphorbol-13-acetate (TPA), 4-(2-hydroxyethyl)-1-piperazineethanesulfonic acid (HEPES), phosphate buffered saline (PBS), trisodium citrate, hydrogen peroxide, hematoxylin, eosin, $MgCl_2$, KCl, phenylmethylsulphonyl fluoride (PMSF), paraformaldehyde, leupeptin, pepstatin A, aprotinin, sodium orthovanadate, β-glycerophosphate, sodium fluoride, dithiothreitol, Triton X-100, anti-iNOS (Sigma–Aldrich, São Paulo, SP, Brazil), xylene, methanol, acetone, (Merck & Co., Inc., Whitehouse Station, NJ, USA), anti-p38, anti-ERK, anti-β-actin, anti-iNOS (Santa Cruz Biotech. Inc., Santa Cruz, CA, USA), anti-COX-2 (Cayman Chemicals, Ann Arbor, MI, USA), anti-phosphorylated (p)-p38(Thr^{180} and Tyr^{182}), anti-p-ERK(Thr^{183} and Tyr^{185}), 5-bromo-4-chloro-3-indolyl phosphate/nitroblue tetrazolium color development substrate (BCIP/NBT) (Promega, Madison, WI, USA), ECL chemiluminescence detection system (GE Healthcare, São Paulo, SP, Brazil), anti-p-CREB(Ser^{133}), anti-p-c-Jun(Ser^{73}), anti-p-p65 NF-κB(Ser^{276}), anti-COX-2 (Cell Signaling Technology, Beverly, MA, USA), Vectastain Elite ABC reagent (Vector Laboratories, Burlingame, CA, USA) and 3,3′-diaminobenzidine (DAB) (Dako, Glostrup, Denmark).

2.6. Statistical analysis

The results are presented as mean ± SEM. The statistical significance between the groups was assessed by means of one-way ANOVA followed by post-hoc Newman-Keuls test. The accepted level of significance for the tests was $P < 0.05$. All tests were carried out using the Statistica software package (StatSoft Inc., Tulsa, OK, USA).

3. Results

3.1. Role of iNOS in TPA-induced ear edema and cellular infiltration

To elucidate the role of iNOS in skin inflammation we subjected WT and iNOS$^{-/-}$ mice to a model of acute skin edema induced by a single topical application of TPA in the ear. A rapid onset and time-dependent induction of edematogenic response was observed in TPA-treated mice. The increase in ear edema was detected after 2 h of TPA treatment, remaining elevated for at least 6 h (Fig. 1A). The calculated area under the curve for the time-dependent TPA-induced ear edema in the WT mice was 1024 ± 96. Nonetheless, we found a reduction in the ear edema elicited by TPA in iNOS$^{-/-}$ mice when compared to the parental strain harboring the intact iNOS gene.

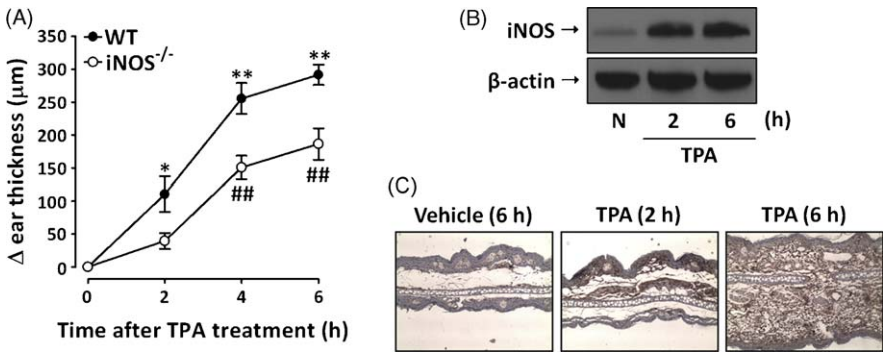

Fig. 1. Involvement of iNOS in TPA-induced ear edema. The skin inflammation was induced by the topical application of TPA (2.5 μg/ear) in the ear of WT and iNOS$^{-/-}$ mice. (A) The edematogenic response was determined by subtracting ear thickness before the TPA challenge from that determined at each time point indicated. The values represent the mean ± S.E.M. ($N = 6$). $^{*}P < 0.05$ and $^{**}P < 0.01$ compared to the basal ear thickness. $^{\#\#}P < 0.01$ compared to the ear thickness of the TPA-treated WT mouse group at the same time point. (B) Representative images of iNOS and β-actin (loading control) immunodetection in the WT mouse ear. (C) Representative images of iNOS immunostaining in the WT mouse ear. Original magnification 200×.

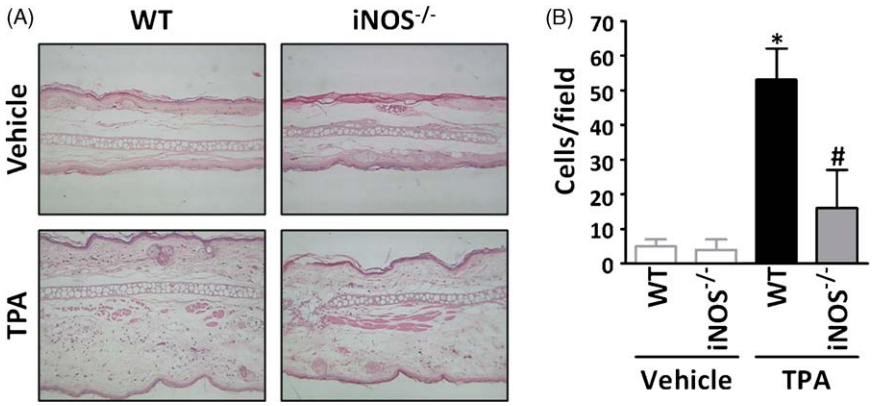

Fig. 2. Involvement of iNOS in TPA-induced cellular infiltration. Histological analysis was performed in the ears of WT and iNOS$^{-/-}$ mice, collected 6 h following the topical application of TPA (2.5 μg/ear). (A) Representative images of hematoxylin and eosin staining in the ear. Original magnification 200×. (B) The number of infiltrating inflammatory cells was determined upon visual inspection in a masked fashion by counting the labeled cells in four non-coincident fields using a counting grid at 400× magnification. The numbers of infiltrating inflammatory cells obtained per field were averaged. The values represent the mean ± S.E.M. ($N = 4$). $^{*}P < 0.05$ compared to vehicle-treated group. $^{\#}P < 0.05$ compared to TPA-treated WT mouse group.

The calculated area under the curve for the time-dependent TPA-induced ear edema in the iNOS$^{-/-}$ mice was 567 ± 101, representing an inhibition of 45%. Notably, the rise in the ear edema is accompanied by a time-dependent increase in the iNOS protein level after TPA treatment in the WT mice (Fig. 1B and C).

Consistently, ear histological analysis revealed a remarkable thickening and cell infiltration in the ear of TPA-treated mice as compared to the skin of vehicle-treated mouse (Fig. 2). The number of inflammatory cells in the skin of TPA-treated WT animals 6 h after topical application was 53 ± 9 cells/field. Notably, we found a significantly impaired infiltration of inflammatory cells in the skin of iNOS$^{-/-}$ mice as compared to WT mice after TPA topical application. The calculated inhibition over TPA-induced cellular influx caused by iNOS genetic deletion was 70%.

3.2. Role of iNOS in TPA-induced COX-2 upregulation

COX-2 can be rapidly induced by inflammatory stimuli, and is often overexpressed in many skin diseases. It has been previously shown that topical application of TPA induces COX-2 upregulation in a NO-dependent manner in the mouse skin *in vivo* [12]. Supporting this data, western blot analysis revealed that topical application of TPA in the ears of WT mice resulted in a dramatic (3.8-fold) upregulation of COX-2 protein expression (Fig. 3A and B).

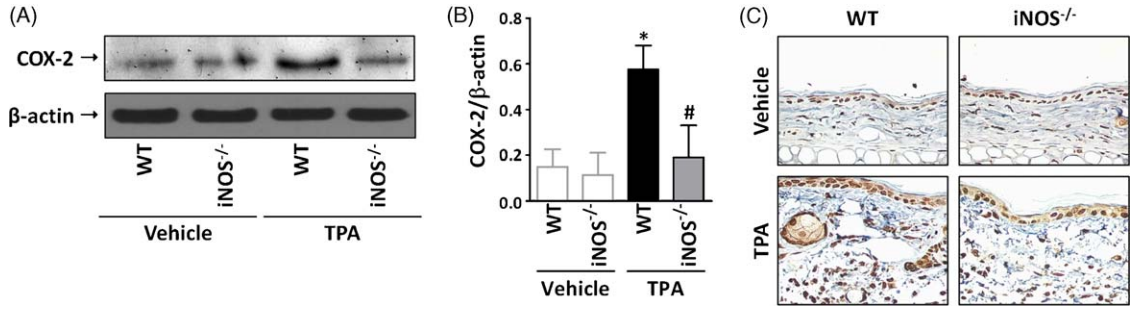

Fig. 3. Involvement of iNOS in TPA-induced COX-2 upregulation. Western blot analysis was performed in the ears of WT and iNOS$^{-/-}$ mice, collected 6 h following the topical application of TPA (2.5 μg/ear). (A) Representative images of COX-2 and β-actin (loading control) immunodetection in the mouse ear. (B) Graphic representation of the COX-2 and β-actin optic densitometry ratio. The values represent the mean ± S.E.M. ($N = 3$). $^{*}P < 0.05$ compared to vehicle-treated group. $^{\#}P < 0.05$ compared to TPA-treated WT mouse group. (C) Representative images of COX-2 immunostaining in the mouse ear. Original magnification 400×.

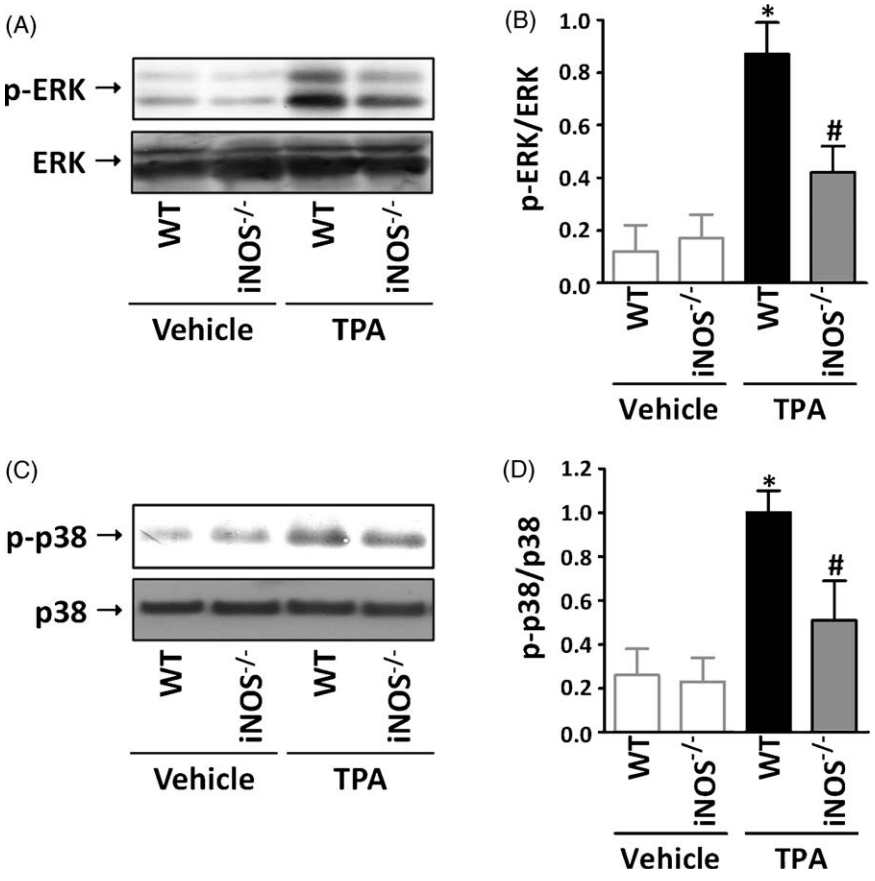

Fig. 4. Involvement of iNOS in TPA-induced MAPK activation. Western blot analysis was performed in the ears of WT and iNOS$^{-/-}$ mice, collected 2 h following the topical application of TPA (2.5 μg/ear). Representative images of (A) p-ERK and (C) p-p38 immunodetection in the mouse ear. Graphic representation of the (B) p-ERK/ERK and (D) p-p38/p38 optic densitometry ratio. The values represent the mean ± S.E.M. ($N = 3$). $^{*}P < 0.05$ compared to vehicle-treated group. $^{\#}P < 0.05$ compared to TPA-treated WT mouse group.

By contrast, the COX-2 upregulation induced by TPA treatment was significantly inhibited in mice lacking the iNOS gene. The calculated inhibition in the TPA-induced COX-2 upregulation found in iNOS$^{-/-}$ mice was 77%. Similarly, immunohistochemical studies revealed that the TPA-induced COX-2 upregulation was inhibited in iNOS$^{-/-}$ mice (Fig. 3C)

3.3. Role of iNOS in TPA-induced intracellular activation

NO has been shown to stimulate MAPKs cascades and, therefore, implicated in regulation of transcription factors, namely, AP-1, NF-κB and CREB [3]. In order to evaluate the participation of iNOS in the TPA-induced intracellular activation, western blot and immunohistochemical analysis were applied. Very low levels of phosphorylated ERK and p38 MAPK are detected in the vehicle-treated mouse ear (Fig. 4). In contrast, in the TPA-treated WT mouse group, a marked activation of ERK (7-fold; Fig. 4A and C) and p38 MAPK (4-fold; Fig. 4B and D) was detected 2 h after TPA treatment. Of interest, the genetic blockage of iNOS largely prevented the activation of ERK and p38 MAPK induced by TPA (inhibition of 60% and 66%, respectively).

Since the transcriptional activity of c-Jun is regulated by phosphorylation at Ser^{63} and Ser^{73}, we then evaluated the phosphorylated level of this transcriptional factor in the mouse ear after TPA treatment. Immunohistochemical studies revealed the presence of p-c-Jun in the skin of vehicle-treated mice. Also, the topical application of TPA in WT mice resulted in a significant increase in the level of p-c-Jun 2 h after treatment, when compared to vehicle-treated mice (Fig. 5). Next, we attempted to outline the role of iNOS in TPA-induced c-Jun phosphorylation. Our results have shown that phosphorylation of c-Jun induced by TPA in the skin was significantly reduced in iNOS$^{-/-}$ mice when compared to WT mice (inhibition of 66%).

We also found that under basal conditions CREB is activated in the mouse skin (Fig. 5). Moreover, a marked increase in p-CREB level is detected 2 h after topical TPA application. Notably, the iNOS genetic deletion inhibited the increase in CREB phosphorylation induced by TPA in the mouse skin when compared to WT mice (inhibition of 30%).

Recent studies have demonstrated that p65 NF-κB phosphorylation is necessary for the transcriptional competence of NF-κB [16]. Upon TPA topical application, the phosphorylated levels of p65 NF-κB subunit was increased in the mouse skin when compared to vehicle-treated mice (Fig. 5). On the other hand, in the iNOS$^{-/-}$ mice the activation of p65 NF-κB induced by TPA was markedly reduced. The blockage of iNOS signaling pathway reduced the increase in the p65 NF-κB phosphorylation induced by TPA by 50%.

4. Discussion

The inflammatory response involves a highly complex interplay between multiple factors at humoral and cellular levels. In the pathogenesis of skin diseases, the immune and inflammatory systems play a pivotal role. Thus, a large production of chemical mediators are produced and released at the site of skin injury [11–14]. In the present study, we have shown that iNOS is an essential component in the TPA-induced skin inflammation. The genetic

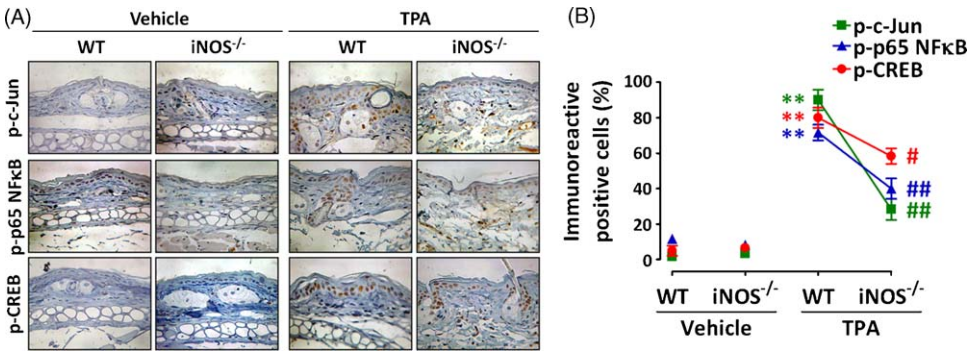

Fig. 5. Involvement of iNOS in TPA-induced transcriptional factors activation. Immunohistochemistry analysis was performed in the ears of WT and iNOS$^{-/-}$ mice, collected 2 h following the topical application of TPA (2.5 μg/ear). (A) Representative images of p-c-Jun, p-p65 NF-κB, and p-CREB immunostaining in the mouse ear. Original magnification 400×. (B) The number of positive cells was determined upon visual inspection in a masked fashion by counting the labeled cells in four non-coincident fields using a counting grid at 400× magnification. The values were expressed as the percentage of positive cells and represent the mean ± S.E.M. ($N = 4$). $^{**}P < 0.01$ compared to vehicle-treated group. $^{\#}P < 0.05$ and $^{\#\#}P < 0.01$ compared to TPA-treated WT mouse group.

ablation of iNOS resulted in a remarkable effect on the inflammatory cascade as indicated by the decrease in the edematogenic response and in the number of infiltrating inflammatory cells in response to TPA in the mouse ear. The inflammatory effects mediated by iNOS seem to be associated with its ability to stimulate the activation of ERK and p38 MAPK, which in turn controls the transcriptional factors, mainly CREB, c-Jun and NF-κB. Notably, we have also reported that iNOS signaling pathways directly participate in TPA-induced COX-2 upregulation.

The NO has been implicated as a key mediator in the microvasculature homeostasis. Under physiological conditions, eNOS-derived NO protects the endothelium from injury and further supports microvascular blood flow by scavenging superoxide, thereby inhibiting neutrophil adhesion [17–19]. Nonetheless, the role of NO in the regulation of microvasculature functions during pathological conditions is still not clear. Whereas some studies have demonstrated that the raise in the NO output by iNOS greatly contributes to the breakdown of the blood-tissue barrier leading to cellular infiltration and plasma protein extravasation; other reports have suggested an entirely opposed effect. For instance, the exposure of leukocytes to high concentrations of NO, as encountered while traversing inflamed vessels, has been shown to boost the production of the chemokine interleukin-8 and the cytokine tumor necrosis factor-α, thus reinforcing a strong chemotactic gradient into damaged tissues [20–23]. Moreover, it has been reported that iNOS activity promotes vascular dilation increasing leukocyte flow in response to infectious stimulus [20]. Recent reports indicate that a lack of iNOS suppresses leukocyte-endothelial cell interactions induced by bacterial endotoxin in the retina and lungs of mice [24–26]. Consistent with these findings, our data clearly demonstrated that genetic deletion of iNOS prevents the cellular infiltration and edema in the skin following TPA challenge. Conversely, there is also evidence suggesting that circulating cytokines and chemokines, acting through activation of iNOS, decrease neutrophil rolling and adhesion to endothelial cells, resulting in the decline of neutrophil migration to the focus of infection [27–29]. The reason for such discrepancy is unknown; however it may be due to differences in the levels of S-nytrosilation, mediated by iNOS-derived NO binding in the cysteine residues of target proteins, in the models applied in each of the studies. Changes in the S-nitrosylation/denitrosylation state have been documented in the physiological [30,31] as well as pathological conditions, where it can reach a hazardous level, a condition known as nitrosative stress [32]. Under such conditions, nitrosylation may promote deleterious oxidative modifications and/or directly inhibit critical protein functions. Indeed, additional studies are necessary to clarify these complex effects mediated by iNOS in the regulation of cellular migration during pathological conditions.

Several independent lines of evidence now suggest that the synthesis of iNOS and COX-2 are elicited with similar time courses, which suggests that both enzymes may interact [33,34]. Regarding the skin, it has been previously reported that iNOS-derived NO modulates the TPA-induced COX-2 upregulation [12]. Although, the molecular mechanisms through which NO affects gene expression are still poorly understood, increasing evidence is accumulating that NO preferentially modulates the activation of transcription factors NF-κB and AP-1, and upstream kinases, including IκB kinase (IKK), ERK and p38 MAPK [35–37]. In fact, in some cells, including human blood mononuclear cells, rat glomerular mesangial cells and mouse keratinocytes, treatment with NO donors such as sodium nitroprusside (SNP), S-nitroso-N-acetylpenicillamine (SNAP) and S-nitrosoglutathione (GSNO) resulted in enhanced binding activity of NF-κB and AP-1 family members [38,39]. Moreover, it has been demonstrated that topical application of NO donors raises the COX-2 levels in the mouse skin, a phenomenon that is markedly inhibited by NF-κB blockers [12]. In the present study, we clearly confirmed and largely extended these previous findings. We were able to show that activation of protein kinases ERK and p38 MAPK, and the transcriptional factors NF-κB, AP-1 and CREB induced by TPA in the mouse skin greatly depends on iNOS. In addition, probably though activation of the DNA-binding activity of NF-κB, AP-1 and CREB, the iNOS modulates the TPA-induced COX-2 upregulation in the mouse skin. Although we have not further analyzed the molecular mechanisms by which iNOS modulate its effects, it can be suggested that nitrosylation of critical cysteines by NO may account for the increase in the transcriptional activity and gene expression in the inflamed skin [3]. However, additional studies are still necessary to confirm this hypothesis.

The current results provide clear functional and molecular evidence indicating that blockage of iNOS function consistently inhibits TPA-induced skin inflammation. Therefore, we suggest that iNOS might constitute a potential and useful therapeutic target for the treatment of various inflammatory cutaneous diseases.

Acknowledgements

This work was supported by grants from the Conselho Nacional de Desenvolvimento Científico e Tecnológico (CNPq), the Coordenação de Aperfeiçoamento de Pessoal de Nível Superior (CAPES), the Programa de Apoio aos Núcleos de Excelência (PRONEX), and

by the Fundação de Apoio a Pesquisa do Estado de Santa Catarina (FAPESC), all from Brazil.

References

[1] Nathan C, Xie QW. Nitric oxide synthases: roles, tolls, and controls. Cell 1994;78:915–8.
[2] Lamas S, Perez-Sala D, Moncada S. Nitric oxide: from discovery to the clinic. Trends Pharmacol Sci 1998;19:436–8.
[3] Beck KF, Eberhardt W, Frank S, Huwiler A, Messmer UK, Muhl H, et al. Inducible NO synthase: role in cellular signalling. J Exp Biol 1999;202:645–53.
[4] Fitzpatrick B, Mehibel M, Cowen RL, Stratford IJ. iNOS as a therapeutic target for treatment of human tumors. Nitric Oxide 2008;19:217–24.
[5] Medeiros R, Prediger RD, Passos GF, Pandolfo P, Duarte FS, Franco JL, et al. Connecting TNF-alpha signaling pathways to iNOS expression in a mouse model of Alzheimer's disease: relevance for the behavioral and synaptic deficits induced by amyloid beta protein. J Neurosci 2007;27:5394–404.
[6] Cauwels A. Nitric oxide in shock. Kidney Int 2007;72:557–65.
[7] Sass G, Koerber K, Bang R, Guehring H, Tiegs G. Inducible nitric oxide synthase is critical for immune-mediated liver injury in mice. J Clin Invest 2001;107:439–47.
[8] Hvid H, Teige I, Kvist PH, Svensson L, Kemp K. TPA induction leads to a Th17-like response in transgenic K14/VEGF mice: a novel in vivo screening model of psoriasis. Int Immunol 2008;20:1097–106.
[9] Kang JS, Yoon WK, Youm JK, Jeong SK, Park BD, Han MH, et al. Inhibition of atopic dermatitis-like skin lesions by topical application of a novel ceramide derivative, K6PC-9p, in NC/Nga mice. Exp Dermatol 2008;17:958–64.
[10] Mueller MM. Inflammation in epithelial skin tumours: old stories and new ideas. Eur J Cancer 2006;42:735–44.
[11] Medeiros R, Otuki MF, Avellar MC, Calixto JB. Mechanisms underlying the inhibitory actions of the pentacyclic triterpene alpha-amyrin in the mouse skin inflammation induced by phorbol ester 12-O-tetradecanoylphorbol-13-acetate. Eur J Pharmacol 2007;559:227–35.
[12] Chun KS, Cha HH, Shin JW, Na HK, Park KK, Chung WY, et al. Nitric oxide induces expression of cyclooxygenase-2 in mouse skin through activation of NF-kappaB. Carcinogenesis 2004;25:445–54.
[13] Cataisson C, Ohman R, Patel G, Pearson A, Tsien M, Jay S, et al. Inducible cutaneous inflammation reveals a protumorigenic role for keratinocyte CXCR2 in skin carcinogenesis. Cancer Res 2009;69:319–28.
[14] Pietrovski EF, Otuki MF, Regoli D, Bader M, Pesquero JB, Cabrini DA, et al. The non-peptide kinin receptor antagonists FR 173657 and SSR 240612: preclinical evidence for the treatment of skin inflammation. Regul Pept 2009;152:67–72.
[15] MacMicking JD, Nathan C, Hom G, Chartrain N, Fletcher DS, Trumbauer M, et al. Altered responses to bacterial infection and endotoxic shock in mice lacking inducible nitric oxide synthase. Cell 1995;81:641–50.
[16] Ghosh S, Karin M. Missing pieces in the NF-kappaB puzzle. Cell 2002;109(Suppl):S81–96.
[17] Gaboury J, Woodman RC, Granger DN, Reinhardt P, Kubes P. Nitric oxide prevents leukocyte adherence: role of superoxide. Am J Physiol 1993;265:H862–7.
[18] Niu XF, Smith CW, Kubes P. Intracellular oxidative stress induced by nitric oxide synthesis inhibition increases endothelial cell adhesion to neutrophils. Circ Res 1994;74:1133–40.
[19] Kubes P, Kanwar S, Niu XF, Gaboury JP. Nitric oxide synthesis inhibition induces leukocyte adhesion via superoxide and mast cells. Faseb J 1993;7:1293–9.
[20] Corriveau CC, Madara PJ, Van Dervort AL, Tropea MM, Wesley RA, Danner RL. Effects of nitric oxide on chemotaxis and endotoxin-induced interleukin-8 production in human neutrophils. J Infect Dis 1998;177:116–26.
[21] Ma P, Cui X, Wang S, Zhang J, Nishanian EV, Wang W, et al. Nitric oxide post-transcriptionally up-regulates LPS-induced IL-8 expression through p38 MAPK activation. J Leukoc Biol 2004;76:278–87.
[22] Muhl H, Chang JH, Huwiler A, Bosmann M, Paulukat J, Ninic R, et al. Nitric oxide augments release of chemokines from monocytic U937 cells: modulation by anti-inflammatory pathways. Free Radic Biol Med 2000;29:969–80.
[23] Van Dervort AL, Yan L, Madara PJ, Cobb JP, Wesley RA, Corriveau CC, et al. Nitric oxide regulates endotoxin-induced TNF-alpha production by human neutrophils. J Immunol 1994;152:4102–9.
[24] Shanley TP, Zhao B, Macariola DR, Denenberg A, Salzman AL, Ward PA. Role of nitric oxide in acute lung inflammation: lessons learned from the inducible nitric oxide synthase knockout mouse. Crit Care Med 2002;30:1960–8.
[25] Okamoto T, Gohil K, Finkelstein EI, Bove P, Akaike T, van der Vliet A. Multiple contributing roles for NOS2 in LPS-induced acute airway inflammation in mice. Am J Physiol Lung Cell Mol Physiol 2004;286:L198–209.
[26] Iwama D, Miyahara S, Tamura H, Miyamoto K, Hirose F, Yoshimura N. Lack of inducible nitric oxide synthases attenuates leukocyte-endothelial cell interactions in retinal microcirculation. Br J Ophthalmol 2008;92:694–8.
[27] Alves-Filho JC, Benjamim C, Tavares-Murta BM, Cunha FQ. Failure of neutrophil migration toward infectious focus in severe sepsis: a critical event for the outcome of this syndrome. Mem Inst Oswaldo Cruz 2005;100(Suppl 1):223–6.
[28] Benjamim CF, Ferreira SH, Cunha FQ. Role of nitric oxide in the failure of neutrophil migration in sepsis. J Infect Dis 2000;182:214–23.
[29] Mestriner FL, Spiller F, Laure HJ, Souto FO, Tavares-Murta BM, Rosa JC, et al. Acute-phase protein alpha-1-acid glycoprotein mediates neutrophil migration failure in sepsis by a nitric oxide-dependent mechanism. Proc Natl Acad Sci USA 2007;104:19595–600.
[30] Stamler JS, Jia L, Eu JP, McMahon TJ, Demchenko IT, Bonaventura J, et al. Blood flow regulation by S-nitrosohemoglobin in the physiological oxygen gradient. Science 1997;276:2034–7.
[31] Mannick JB, Hausladen A, Liu L, Hess DT, Zeng M, Miao QX, et al. Fas-induced caspase denitrosylation. Science 1999;284:651–4.
[32] Dalle-Donne I, Rossi R, Colombo G, Giustarini D, Milzani A. Protein S-glutathionylation: a regulatory device from bacteria to humans. Trends Biochem Sci 2009.
[33] Appleton I, Tomlinson A, Willoughby DA. Induction of cyclo-oxygenase and nitric oxide synthase in inflammation. Adv Pharmacol 1996;35:27–78.
[34] Misko TP, Trotter JL, Cross AH. Mediation of inflammation by encephalitogenic cells: interferon gamma induction of nitric oxide synthase and cyclooxygenase 2. J Neuroimmunol 1995;61:195–204.
[35] Wang S, Zhang J, Zhang Y, Kern S, Danner RL. Nitric oxide-p38 MAPK signaling stabilizes mRNA through AU-rich element-dependent and -independent mechanisms. J Leukoc Biol 2008;83:982–90.
[36] Min KS, Kim HI, Chang HS, Kim HR, Pae HO, Chung HT, et al. Involvement of mitogen-activated protein kinases and nuclear factor-kappa B activation in nitric oxide-induced interleukin-8 expression in human pulp cells. Oral Surg Oral Med Oral Pathol Oral Radiol Endod 2008;105:654–60.
[37] Taimor G, Rakow A, Piper HM. Transcription activator protein 1 (AP-1) mediates NO-induced apoptosis of adult cardiomyocytes. Faseb J 2001;15:2518–20.
[38] Lander HM, Sehajpal P, Levine DM, Novogrodsky A. Activation of human peripheral blood mononuclear cells by nitric oxide-generating compounds. J Immunol 1993;150:1509–16.
[39] Peng HB, Rajavashisth TB, Libby P, Liao JK. Nitric oxide inhibits macrophage-colony stimulating factor gene transcription in vascular endothelial cells. J Biol Chem 1995;270:17050–5.